Letter

Susceptibility indicator for chiral topological orders emergent from correlated fermions

Rui Wang,[1,2,3] Tao Yang,[1] Z. Y. Xie,[4,*] Baigeng Wang,[1,2,†] and X. C. Xie[5,6,7]

[1]*National Laboratory of Solid State Microstructures and Department of Physics, Nanjing University, Nanjing 210093, China*

[2]*Collaborative Innovation Center for Advanced Microstructures, Nanjing University, Nanjing 210093, China*

[3]*Hefei National Laboratory, Hefei 230088, China*

[4]*Department of Physics, Renmin University of China, Beijing 100872, China*

[5]*International Center for Quantum Materials, School of Physics, Peking University, Beijing 100871, China*

[6]*Collaborative Innovation Center of Quantum Matter, Beijing 100871, China*

[7]*CAS Center for Excellence in Topological Quantum Computation, University of Chinese Academy of Sciences, Beijing 100190, China*

(Received 31 January 2023; revised 1 June 2024; accepted 5 June 2024; published 18 June 2024)

Chiral topological orders formed in correlated fermion systems have been widely explored. However, the mechanism of how they emerge from interacting fermions is still unclear. Here, we propose a susceptibility condition. Under this condition, we show that chiral topological orders can spontaneously take place in correlated fermion systems. The condition leads to a low-energy effective theory of bosons with strong frustration, mimicking flat-band systems. The frustration then melts the long-range orders and results in topological orders with time-reversal symmetry breaking. We apply the theory to strongly correlated semiconductors doped to the metallic phase. An excitonic topological order with semionic excitations and a chiral excitonic edge state is revealed. We also discuss the application to frustrated magnets. The theory predicts a chiral spin-liquid state, which is numerically confirmed by our tensor network calculations. These results demonstrate an indicator for chiral topological orders, which bridges the existing gap between interacting fermions and correlated topological matter.

DOI: 10.1103/PhysRevB.109.L241113

Introduction. Chiral topological orders (TOs) breaking time-reversal symmetry (TRS) has been a prominent topic over the last decades [1,2], and its discovery in fractional quantum Hall (FQH) systems [3–5] invokes some of the most fundamental concepts in modern condensed matter physics [6–10]. Chiral topological orders are usually formed in correlated fermion systems. For example, FQH states are generated from correlated electron states in Landau levels [3–5]; chiral spin liquids (CSLs) are formed in frustrated magnets [11–13] or Mott insulators [14], which again originate from strongly correlated electronic materials. Moreover, the chiral excitonic topological order (ETO) recently revealed in InAs/GaSb quantum wells also emerges from interacting electron-hole bilayers [15]. These facts suggest there might be an underlying mechanism of chiral TOs accounting for their emergence from interacting fermions, which is yet to be addressed.

A convenient starting point to study interacting fermions is the Fermi liquid [16]. The instabilities of Fermi liquids provide a unified description of many long-range ordered states [17–19], including superconductors, charge density waves, and magnetic orders, which can be understood as the condensation of bosons in corresponding channels. However, chiral TOs are disordered and characterized by long-range quantum entanglement, in stark contrast with ordered states [20–22]. Therefore, it is a great challenge to find out their connections with correlated fermion systems, which demand different developments beyond the conventional theory of Fermi-liquid instability.

Two-dimensional (2D) interacting fermions are generally described by $H = H_0 + H_I$, where $H_0 = \sum_{\mathbf{r},\alpha} c^\dagger_{\mathbf{r}\alpha} h_\alpha(-i\boldsymbol{\nabla}) c_{\mathbf{r},\alpha}$ and $h_\alpha(-i\boldsymbol{\nabla}) = |\mathbf{k}|^2/2m_\alpha$ is the kinetic energy, with $\alpha = 1, \ldots, N$ being the band and spin indices. The fermion-fermion interaction reads as $H_I = \sum_{\mathbf{r},\mathbf{r}',\alpha,\beta} V(\mathbf{r}-\mathbf{r}') c^\dagger_{\mathbf{r},\alpha} c_{\mathbf{r},\beta} c^\dagger_{\mathbf{r}',\beta} c_{\mathbf{r}',\alpha}$, where $\alpha \neq \beta$ is allowed. $\mathbf{g} = \{m_\alpha, \mu, \ldots\}$ denotes the model parameters, including the mass m_α and the chemical potential μ. The key quantity indicating possible instabilities is the susceptibility $\chi_{\mathbf{g},\alpha\beta}(q) = -\sum_k G_{0,\alpha}(k) G_{0,\beta}(k+q)$ [17,18], with $G_{0,\alpha}(k)$ the bare Green's function of fermions and $k = (\mathbf{k}, i\omega_n)$. At the random phase approximation level, the interaction is renormalized as $V'(q) = V(\mathbf{q})/[1 + V(\mathbf{q})\chi_{\mathbf{g},\alpha\beta}(q)]$. It is known that, when the condition $1 + V(\mathbf{q})\chi_{\mathbf{g},\alpha\beta}(\mathbf{q}, 0) = 0$ is satisfied at a single momentum point $\mathbf{q} = \mathbf{Q}$, the divergence indicates the formation of boson condensates or long-range orders.

In this Letter, we focus on an intriguing question, i.e., what is the fate of bosons if the above condition is simultaneously satisfied by an infinite number of points on a momentum loop, i.e.,

$$1 + V(\mathbf{q})\chi_{\mathbf{g},\alpha\beta}(\mathbf{q}, 0) = 0, \quad \forall \mathbf{q} \in S^1, \tag{1}$$

*Contact author: qingtaoxie@ruc.edu.cn

†Contact author: bgwang@nju.edu.cn

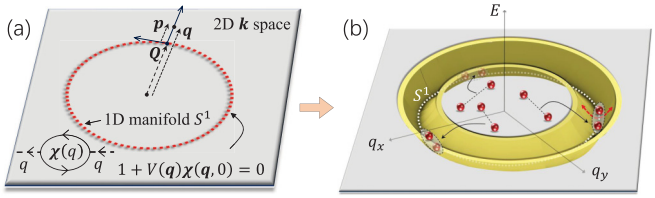

FIG. 1. (a) The correlated fermion systems satisfying the condition in Eq. (1) on a 1D manifold $\Lambda = S^1$ embedded in 2D $\mathbf{k}$ space. (b) Under Eq. (1), a low-energy effective theory takes place, which describes the fermion pairs on a moat-shaped band with the energy minima on S^1.

given S^1 a 1D loop embedded in 2D momentum space with radius Q, as indicated by Fig. 1(a). Equation (1) essentially implies that bosons have an equal tendency to condense on each point of S^1, implying a strong frustration effect. We show that Eq. (1) generates a low-energy effective theory describing interacting bosons on a moat-shaped band [23–26], as shown in Fig. 1(b). The emergent physics mimics the flat-band systems [27–30] along S^1 in a bosonic version, finally resulting in chiral TOs with TRS breaking. We apply the theory to study strongly correlated semiconductors doped to the metallic phase, which satisfies the susceptibility condition in the particle-hole channel. Another ETO state is revealed, which exhibits semionic anyons in the bulk and chiral excitonic edge state [15]. More interestingly, by applying the theory to frustrated quantum magnets, we predict a chiral spin liquid, which is numerically confirmed by our tensor network calculations. These results reveal the long-desired connections between chiral TOs and interacting fermions.

Emergence of chiral TO under the susceptibility condition. We assume Eq. (1) is satisfied at $\mathbf{g} = \mathbf{g}_{\rm cri}$ and study the general fermion model. By introducing the auxiliary bosons $O_{\mathbf{r},\alpha\beta}$, H_I can be decomposed into the boson-fermion interaction,

$$S_I = \int d\tau \sum_{\mathbf{r},\mathbf{r}'} [O^\dagger_{\mathbf{r},\alpha\beta} V(\mathbf{r}-\mathbf{r}') c^\dagger_{\mathbf{r}',\beta} c_{\mathbf{r}',\alpha} + \text{H.c.}] + \cdots, \quad (2)$$

where the repeated indices are summed and "$\cdots$" denotes the boson bilinear terms. Introducing the operator $b_{\mathbf{r},a} \equiv b_{\mathbf{r},\alpha\beta} = \sum_{\mathbf{r}'} V(\mathbf{r}-\mathbf{r}') O_{\mathbf{r}',\alpha\beta}$, where a is the boson flavor with $a = 1, \ldots, N^2$, and integrating out the fermions [31,32], we obtain $Z = \int Db^\star Dbe^{-S_{\rm eff}}$. The effective action of the bosons $S_{\rm eff}$ reads as

$$S_{\rm eff} = -\text{Tr}\ln[-G^{-1}(\tau,\mathbf{r})] - \text{Tr}[b^\dagger_{\mathbf{r}} V^{-1}(\mathbf{r}-\mathbf{r}') b_{\mathbf{r}'}], \quad (3)$$

where $b_{\mathbf{r}}$ is the matrix with entries $b_{\mathbf{r},\alpha\beta}$. $G^{-1}(\tau,\mathbf{r}) = G_0^{-1}(\tau,\mathbf{r}) - \Sigma(\tau,\mathbf{r})$ is the renormalized Green's function, with $G_0^{-1}(\tau,\mathbf{r}) = [-\partial_\tau - h(-i\nabla)]$. $\Sigma(\tau,\mathbf{r}) = b_{\mathbf{r}} + b^\dagger_{\mathbf{r}}$ is the self-energy, which can be treated perturbatively at $\mathbf{g} = \mathbf{g}_{\rm cri}$ [31].

To second-order perturbation, the action of bosons is obtained as $S_{0,\rm eff} = \sum_a S^{(a)}_{0,\rm eff}$, and the a-flavor sector is described by

$$S^{(a)}_{0,\rm eff} = -\sum_q [\chi_{\mathbf{g},a}(q) + V^{-1}(\mathbf{q})] b^\dagger_{q,a} b_{q,a}. \quad (4)$$

The saddle-point equation, $\delta S^{0,(a)}_{\rm eff}/\delta b_{q,a} = 0$, can be derived, which exactly reproduces the identity in Eq. (1). Thus, Eq. (1) states that there are an infinite number of saddle-point solutions and quantum fluctuations are non-negligible. Thus, we take into account the long-wave fluctuations around the saddle points. A generic momentum $\mathbf{q}$ can be measured in local Cartesian coordinates with the origin $\mathbf{Q}$ and the unit vector tangential to S^1 [Fig. 1(a)], i.e., $\mathbf{p} = \mathbf{q} - \mathbf{Q}$. Then, making an expansion with respect to $|\mathbf{p}|$ and $i\nu_n$ leads to the low-energy effective theory [32],

$$S^{(a)}_{0,\rm eff} = \sum_{i\nu_n,\mathbf{q}} \left[-i\nu_n + \frac{(|\mathbf{q}|-Q)^2}{2\tilde{m}_a} - \tilde{\mu}_a \right] b^\dagger_{q,a} b_{q,a}, \quad (5)$$

where $\tilde{m}_a$, $\tilde{\mu}_a$ are the effective mass and chemical potential of the a-flavor bosons, which are dependent on $\mathbf{g}$. Interestingly, we observe from Eq. (5) that the kinetic energy of bosons is minimized for $|\mathbf{q}| = Q$, namely, on the loop S^1. Moreover, quadratic dispersion takes place for $\mathbf{q}$ deviating from S^1, leading to the moat band shown in Fig. 1(b). For $\mathbf{g} = \mathbf{g}_{\rm cri}$ where Eq. (1) is satisfied, $\tilde{\mu}_a = 0$ can be rigorously proved [32]. This is a reflection of the fact that the bosons are about to condense at $\mathbf{g} = \mathbf{g}_{\rm cri}$. However, as will be clear in the following, the condensation will be suppressed by a quantum fluctuation.

To the fourth order, similar derivations as above lead to the following effective action:

$$S^{(a)}_{I,\rm eff} = U_a \sum_{q_1,q_2,q_3} b^\dagger_{q_1,a} b_{q_1-q_2+q_3,a} b^\dagger_{q_3,a} b_{q_2,a}. \quad (6)$$

The coupling constant $U_a = 4\sum_k G^2_{0,\alpha}(k) G^2_{0,\beta}(k)$ is generally positive. Collecting both Eqs. (5) and (6), we arrive at the effective Hamiltonian of bosons,

$$H_{\rm eff} = \sum_{\mathbf{q}} \left[\frac{(|\mathbf{q}|-Q)^2}{2\tilde{m}} - \tilde{\mu} \right] b^\dagger_{\mathbf{q}} b_{\mathbf{q}} + U \sum_{\mathbf{r}} b^\dagger_{\mathbf{r}} b_{\mathbf{r}} b^\dagger_{\mathbf{r}} b_{\mathbf{r}}, \quad (7)$$

where the flavor a is implicit. $\tilde{\mu}$ can be formally canceled by shifting the zero of energy. Clearly, Eq. (7) describes interacting bosons on the moat band, as indicated in Fig. 1(b).

We now examine the possible ground state of Eq. (7). Due to the flatness of the moat band along S^1, the interaction U plays the dominant role. In this case, the system can lower the energy cost from U by statistical transmutations via the flux attachment [33–35]. Technically, we represent the bosons as composite fermions (CFs) attached to a 1-flux quantum [36–42], i.e., $\Psi_b(\mathbf{r}_1,\ldots,\mathbf{r}_N) = \Psi_f(\mathbf{r}_1,\ldots,\mathbf{r}_N) e^{i\sum_{i<j}\arg[\mathbf{r}_i-\mathbf{r}_j]}$. Although the fluxes cost the kinetic energy $\langle\Psi_b|H_K|\Psi_b\rangle$, where $H_K = (|\mathbf{q}|-Q)^2/2\tilde{m}$, the interaction energy from U, which plays the dominant role here, is significantly reduced in such a representation because of the antisymmetric nature of $\Psi_f(\mathbf{r}_1,\ldots,\mathbf{r}_N)$. Hence, the fluxes that break TRS could be spontaneously generated, as they can further lower the system energy.

The next step is to look for the ground state wave function, $\Psi_f(\mathbf{r}_1,\ldots,\mathbf{r}_N)$. Using $\Psi_b(\mathbf{r}_1,\ldots,\mathbf{r}_N) = \Psi_f(\mathbf{r}_1,\ldots,\mathbf{r}_N) e^{i\sum_{i<j}\arg[\mathbf{r}_i-\mathbf{r}_j]}$, the Hamiltonian in the fermionic basis describes composite fermions coupled to the Chern-Simons (CS) flux $B_{\rm CS} = 2\pi n$ [39–42], where n is the fermion density [43]. Consequently, Landau quantization is formed, and the ground state in terms of $\Psi_f(\mathbf{r}_1,\ldots,\mathbf{r}_N)$ is

obtained to be the lowest Landau level state. Therefore, we arrive at the bosonic ground state wave function [32],

$$\Psi_b(\mathbf{r}_1,\ldots,\mathbf{r}_N)=\frac{1}{\sqrt{N!}}\det_{m,j}\left[\chi^l_m(z_j)\right]e^{i\sum_{i<j}\arg[\mathbf{r}_i-\mathbf{r}_j]}, \quad (8)$$

where $\chi^l_m(z_j)=A_{l,m}(\frac{z}{l_B})^m e^{\frac{|z|^2}{4l_B^2}}L_l^{(m)}[\frac{|z|^2}{2l_B^2}]$ is the eigenstate of the lth Landau level (l determined by n [32]) with the normalization factor $A_{l,m}$ and the complex coordinate z. Equation (8) describes the lowest Landau level fully filled by composite fermions, which are bosons attached to 1-flux quanta.

The state in Eq. (8) is essentially a chiral bosonic topological order, as it can be equivalently understood as a $\nu=1/2$ bosonic FQH [32] due to the following reason. Starting from a $\nu=1/2$ bosonic FQH under an intrinsic CS field $B_\perp$ and $\nu=\phi_D\rho_0/B_\perp=1/2$, where ϕ_D is the flux quantum and ρ_0 the particle number, and regarding the boson as the composite fermion attached to 1-flux quantum, then the effective field seen by the composite fermions is $B_{\rm CS}=B_\perp-\phi_D\rho_0=B_\perp/2$. Hence, the fermion filling factor is $\nu_{\rm eff}=\phi_D\rho_0/B_{\rm eff}=1$, leading to the fully filled Landau level state in Eq. (8).

The energy of the state in Eq. (8) can then be evaluated via $\langle\Psi_b|H_K|\Psi_b\rangle$, leading to $E_{\rm TO}=\langle\Psi_b|[\frac{(|\mathbf{q}|-Q)^2}{2\tilde{m}}]|\Psi_b\rangle=\frac{\pi^2n^2}{2\tilde{m}Q^2}\log^2\frac{4n}{Q^2}$ [24,32]. Remarkably, in the low-density regime $n\to 0$, $E_{\rm TO}$ has a lower energy than that of all the condensates proposed to date [32], including the Fulde-Ferrell-Larkin-Ovchinnikov (FFLO) ($E_{\rm FFLO}\propto n$ [44,45]) and the fragmented condensate ($E_{\rm frag}\propto n^{4/3}$ [46]). Notably, the energetics obtained here is confirmed by a recent Monte Carlo simulation [47].

Last, we recall that $\tilde{\mu}=0$ has been proved in Eq. (5) for $\mathbf{g}=\mathbf{g}_{\rm cri}$ [32] and $n\propto 2\sqrt{\tilde{\mu}}$ [15]. Thus, $n\to 0$ is always satisfied for $\mathbf{g}\simeq\mathbf{g}_{\rm cri}$. Therefore, we arrive at the key conclusion of this Letter, i.e., the chiral TO described by Eq. (8) will always emerge as the possible ground state, at least in a finite parameter region around $\mathbf{g}\simeq\mathbf{g}_{\rm cri}$ where Eq. (1) is satisfied.

Application 1: Excitonic topological order. We now apply the above general theory to study strongly correlated doped semiconductors. The Hamiltonian is given by $H=H_0+H_I$, where $H_0=\sum_{\mathbf{k},n,\sigma}\epsilon_n(\mathbf{k})c^\dagger_{n,\mathbf{k},\sigma}c_{n,\mathbf{k},\sigma}$ with spin σ. The conduction and valence bands are described by $\epsilon_\pm(\mathbf{k})=\pm k^2/2m\pm D/2-\mu_0$, where μ_0 is the chemical potential and D is the band offset. We are interested in the doped metallic state with the electron (or hole) Fermi surface, i.e., $0<D<2|\mu_0|$, as indicated by Fig. 2(a). On top of H_0, we consider the short-range interband interaction between the electrons, i.e., $H_I=V\sum_{\mathbf{k},\mathbf{k}',\mathbf{q}}\sum_{\sigma,\sigma'}c^\dagger_{+,\mathbf{k}+\mathbf{q},\sigma}c_{+,\mathbf{k},\sigma}c^\dagger_{-,\mathbf{k}'-\mathbf{q},\sigma'}c_{-,\mathbf{k}',\sigma'}$. The intraband interaction is negligible as it only modifies the band dispersion via the mass renormalization.

Even if at low temperatures, there are virtual processes where electrons are excited to the conduction band above the Fermi level, leaving hole states in the valence band, as indicated by the dashed arrows in Fig. 2(a). For strong V, the electrons and the holes can form excitons. When the binding energy overcomes the excitation energy, such virtual processes will be relevant, leading to the condensation of excitons, i.e., excitonic insulators (EIs). In conventional mean-field theory [32], we define the excitonic order parameter as $\Delta_{\tilde{\mathbf{q}}}=V\sum_{\mathbf{p}}\langle c^\dagger_{+,\mathbf{p},\sigma}c_{-,\mathbf{p}-\tilde{\mathbf{q}},\sigma}\rangle$ where $\tilde{\mathbf{q}}$ is the net exciton momentum. By solving the mean-field equations, the order parameter $\Delta_{\tilde{\mathbf{q}}}$ is self-consistently determined. The solution $\Delta_{\tilde{\mathbf{q}}}=0$ simply describes the electron (or hole) gas without ordering. For the solutions where $\Delta_{\tilde{\mathbf{q}}}$ is maximized at $|\tilde{\mathbf{q}}|=0$, the excitons intend to exhibit zero net momentum. Such a condensate is referred to as the zero-momentum EI, contrary to the condensate at finite momentum, i.e., the FFLO state.

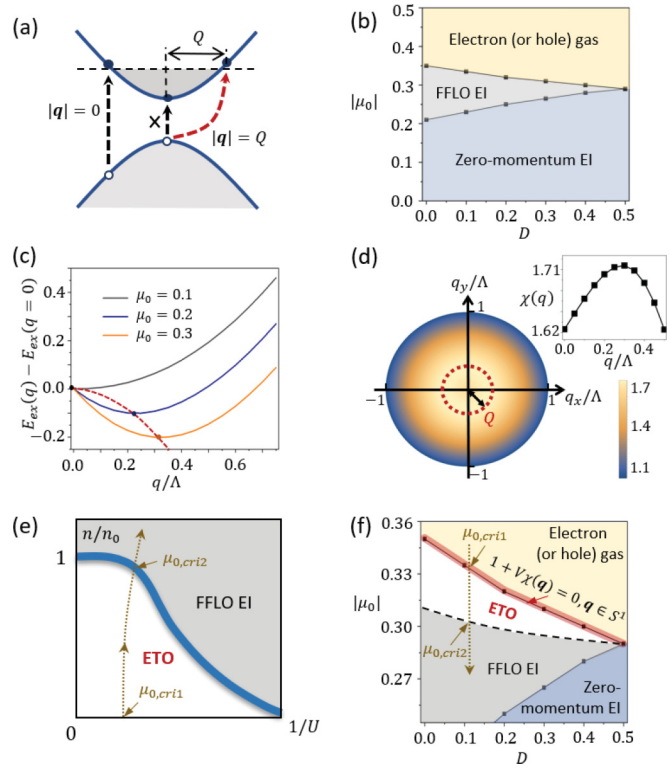

FIG. 2. (a) Plot of a semiconductor doped to the metallic phase, with an implicit energy cutoff $W=\Lambda^2/2m$. The dashed arrows denote the excitation of electron-hole pairs. (b) The calculated mean-field phase diagram. D and $|\mu_0|$ are in units of W. A strong interaction V is required to obtain the EIs, and $V/W=1$ is used in (b). (c) The calculated exciton dispersion for different values of μ_0 and $D=0.2$. The dashed red curve denotes the dispersion minimum with changing μ_0. (d) The density plot of the susceptibility in the particle-hole channel. The inset shows its dependence on q. (e) The phase diagram of the boson model in Eq. (7). (f) The zoom-in phase diagram obtained after considering the frustration effect. The parameters are the same with (b). The red thick curve denotes the critical regime where Eq. (1) is satisfied. With varying the fermion parameters along the yellow dashed line, the parameters of the boson theory in Eq. (7) evolve along the yellow trajectory in (e).

The mean-field phase diagram with varying $|\mu_0|$ and D is shown in Fig. 2(b). As shown, in a strongly doped regime with large μ_0, the system remains as the electron (or hole) gas, because of the dominant excitation energy. For smaller μ_0, the binding energy slightly overcomes the excitation energy. In this case, only the process indicated by the red dashed arrow in Fig. 2(a) becomes relevant, as it has the lowest-energy cost. Clearly, the excitons formed in this channel exhibit finite momenta, thus leading to the FFLO EI after condensation, as shown by Fig. 2(b). With further lowering $|\mu_0|$, the binding energy becomes dominant, so that zero-momentum excitons

can be readily formed, as indicated by the $|\mathbf{q}| = 0$ scattering channel in Fig. 2(a). This leads to the zero-momentum EI in Fig. 2(b).

We then examine the excitation energy as a function of the exciton momentum $\mathbf{q}$. From Fig. 2(a), we observe that it decreases from $|\mathbf{q}| = 0$, and reaches the minimum at $|\mathbf{q}| = Q$. This fact is further manifested by the exciton energy E_{ex}, which can evaluated by minimizing $W_{\text{ex}} = \langle \text{FS}|\Delta_{\mathbf{p}}[H - E_{\text{ex}}(\mathbf{p})]\Delta_{\mathbf{p}}^{\dagger}|\text{FS}\rangle$, where $\Delta_{\mathbf{p}}^{\dagger} = \sum_{\mathbf{k}} \phi_{\mathbf{p}}(\mathbf{k}) c_{+,\mathbf{k},\sigma}^{\dagger} c_{-,\mathbf{p}-\mathbf{k},\sigma}$ with the variation parameter $\phi_{\mathbf{p}}(\mathbf{k})$, and $|\text{FS}\rangle$ denotes the Fermi sea [32]. As shown in Fig. 2(c), for the metallic states, the calculated exciton dispersion exhibits a minimum at finite momentum, leading to the moatlike band of excitons, as that in Fig. 1(b). This indicates that there emerges a frustrated ordering tendency along S^1.

We further calculate the susceptibility $\chi(\mathbf{q}, 0)$ in the particle-hole channel. As shown by Fig. 2(e), $\chi(\mathbf{q}, 0)$ exhibits the same maxima along a momentum loop, as indicated by the red dashed circle. Hence, for a proper parameter $\mathbf{g} = \mathbf{g}_{\text{cri}}$, $1 + V(\mathbf{q})\chi(\mathbf{q}, 0) = 0$ can be satisfied by all $\mathbf{q} \in S^1$, leading to correlated excitons on the moat band [32]. Hence, a chiral TO formed by excitons, i.e., the ETO, should emerge as the ground state for $\mathbf{g} \sim \mathbf{g}_{\text{cri}}$ according to our theory.

A comparison of the energetics between the boson condensates and the ETO leads to the phase diagram corresponding to Eq. (7), as shown in Fig. 2(e). In terms of the original fermion model, we gradually decrease μ_0 along the dashed line in Fig. 2(f). For $\mu_0 = \mu_{0,\text{cri1}}$, where the susceptibility condition is satisfied, $\tilde{\mu} \sim 0$ in Eq. (7), thus the density $n \sim 0$, as discussed above. With further decreasing μ_0, n increases and moves along the dashed trajectory in Fig. 2(e). The system stays in the ETO state until the trajectory crosses the ETO-FFLO boundary at $\mu_0 = \mu_{0,\text{cri2}}$. This determines the ETO region of the phase diagram in Fig. 2(f) Thus, the quantum fluctuation results in a translationally invariant, long-range quantum entangled chiral excitonic state [15,48,49].

Application 2: Chiral spin liquid and numerical evidence. Our theory can also be applied to predict chiral spin liquids in frustrated magnets. We consider the spin-1/2 J_1–J_2–J_3 XY model on a square lattice, which satisfies the susceptibility condition as will be shown below. The model is defined as $H = \sum_{\mathbf{r},\mathbf{r}'} (J_{\mathbf{r},\mathbf{r}'}/2)(S_{\mathbf{r}}^x S_{\mathbf{r}'}^x + S_{\mathbf{r}}^y S_{\mathbf{r}'}^y)$ where the sum evolves the first, second, and third nearest-neighbor bonds. We fermionize the quantum spin model using the 2D Jordan-Wigner transformation [33–35,40–42], which transform the spin operator into fermions and the lattice gauge field. The lattice gauge field has two effects. One is to generate fluxes that minimize the energy of fermions, and the other is to mediate fermion-fermion interactions. Focusing on $J_3 = J_2/2$ and gradually increasing J_2, we plot the single-particle dispersion of the fermions in Figs. 3(a)–3(c). As shown, the Dirac fermion states emerge, and the chemical potential μ_0 gradually moves away from the Dirac points with increasing J_2. For small J_2, the gauge-mediated fermion-fermion interaction has been shown to induce pairing of fermions, whose condensation leads to Néel order [41,42], while for large J_2, another Fermi pocket emerges around the Γ point [Fig. 3(c)]. Then, the

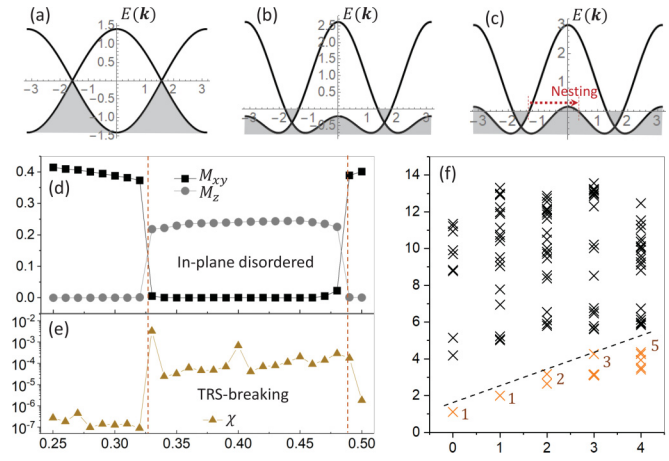

FIG. 3. (a)–(c) The dispersion of fermions along $k_x = k_y$ after a 2D Jordan-Wigner transformation of the J_1–J_2–J_3 XY square model. $J_2/J_1 = 0, 0.4, 0.52$ for (a)–(c), respectively. (d) The calculated in-plane M_{xy} and out-of-plane M_z magnetization with increasing J_2/J_1. (e) The calculated chirality order $\chi = \langle \mathbf{S}_1 \cdot (\mathbf{S}_2 \times \mathbf{S}_3) \rangle$ with $\mathbf{S}_{1,2,3}$ the spin operator defined on three sites of a square plaquette. (f) The entanglement spectrum as a function of k_y. $J_2/J_1 = 0.4$ and k_y is in units of $2\pi/5$. The bond dimension is $D = 10$ in the calculations.

Fermi-surface nesting would favor spin density waves [38]. Interestingly, for intermediate J_2 [Fig. 3(b)], the same low-energy physics as that of the ETO example [Fig. 2(a)] occurs, and the susceptibility condition is satisfied [32]. Therefore, a chiral TO is expected to take place in between two magnetically ordered states.

We then use tensor network calculations [50–62] to simulate the ground state. As shown in Fig. 3(d), in between two in-plane magnetic orders, an intermediate phase ($0.33 \lesssim J_2/J_1 \lesssim 0.49$) occurs, which is completely free from any in-plane ordering. The chirality order also shows a significant enhancement in this region, clearly indicating the spontaneous breaking of TRS. Moreover, the entanglement spectrum exhibits the level counting, $1, 1, 2, 3, 5 \ldots$ [Fig. 3(f)], consistent with the $\text{SU}(2)_1$ conformal field theory, implying the existence of the chiral edge state. These data offer strong evidence for the chiral spin-liquid state, justifying our analytic predictions.

Summary and discussion. The ETO is a chiral bosonic TO exhibiting semionic excitations in the bulk and chiral excitonic edge states [15,32]. Experimental evidence was recently reported in the semimetal phase of InAs/GaSb quantum wells [15,48,49] with a density imbalance [63]. Here, we reveal that ETO can even be formed in the metallic phase of doped semiconductors. In this case, a strong interaction V comparable to the bandwidth W is desired. The twisted TMD bilayers provide a promising platform, which can realize semiconductors with strong correlation and remarkably flat bands [64]. Therefore, our theory could have intimate connections with the recently reported fractional quantum anomalous Hall states in the twisted moiré systems [65–68].

The mechanism revealed here applies to correlated fermionic systems, in which the number of bosons depends on how many fermions are paired. In this case, the

system can always lower its energy at the optimal density [15] where the lowest Landau level is fully filled. In contrast, for bosons with fixed density on a moat band, generic filling of the Landau level is likely. Consequently, metallic states with quasi-long-range order are expected [23]. The proposed mechanism may also be used to predict other chiral TOs, such as fractional Chern insulators [27,28]. The generalization to TRS-preserving TOs and non-Abelian TOs is also an interesting direction.

Acknowledgments. R.W. acknowledges Tigran Sedrakyan, Qianghua Wang, Rui-Rui Du, Lingjie Du, and Y. X. Zhao for fruitful discussions. This work was supported by the National R&D Program of China (Grants No. 2023YFA1406500 and No. 2022YFA1403601), the National Natural Science Foundation of China (Grants No. 12322402 and No. 12274206), the Innovation Program for Quantum Science and Technology (Grant No. 2021ZD0302800), and the Xiaomi Foundation.

[1] V. Kalmeyer and R. B. Laughlin, Phys. Rev. Lett. **59**, 2095 (1987).
[2] X. G. Wen, F. Wilczek, and A. Zee, Phys. Rev. B **39**, 11413 (1989).
[3] D. C. Tsui, H. L. Stormer, and A. C. Gossard, Phys. Rev. Lett. **48**, 1559 (1982).
[4] R. B. Laughlin, Phys. Rev. Lett. **50**, 1395 (1983).
[5] X. G. Wen, Adv. Phys. **44**, 405 (1995).
[6] X. G. Wen, Phys. Rev. B **40**, 7387(R) (1989).
[7] E. Witten, Commun. Math. Phys. **117**, 353 (1988).
[8] D. Arovas, J. R. Schrieffer, and F. Wilczek, Phys. Rev. Lett. **53**, 722 (1984).
[9] X.-G. Wen and Q. Niu, Phys. Rev. B **41**, 9377 (1990).
[10] A. Kitaev and J. Preskill, Phys. Rev. Lett. **96**, 110404 (2006).
[11] L. Balents, Nature (London) **464**, 199 (2010).
[12] Y. Zhou, K. Kanoda, and T.-K. Ng, Rev. Mod. Phys. **89**, 025003 (2017).
[13] Y.-C. He, D. N. Sheng, and Y. Chen, Phys. Rev. Lett. **112**, 137202 (2014).
[14] B. Bauer, L. Cincio, B. P. Keller, M. Dolfi, G. Vidal, S. Trebst, and A. W. W. Ludwig, Nat. Commun. **5**, 5137 (2014).
[15] R. Wang, T. A. Sedrakyan, L. Du, B. Wang, and R.-R. Du, Nature (London) **619**, 57 (2023).
[16] L. D. Landau, Sov. Phys. JETP **3**, 920 (1956).
[17] H. v. Löhneysen, A. Rosch, M. Vojta, and P. Wölfle, Rev. Mod. Phys. **79**, 1015 (2007).
[18] C. Honerkamp, M. Salmhofer, N. Furukawa, and T. M. Rice, Phys. Rev. B **63**, 035109 (2001).
[19] C. Wu, K. Sun, E. Fradkin, and S.-C. Zhang, Phys. Rev. B **75**, 115103 (2007).
[20] X.-G. Wen, Science **363**, eaal3099 (2019).
[21] X. Chen, Z. C. Gu, and X. G. Wen, Phys. Rev. B **82**, 155138 (2010).
[22] M. Levin and X. G. Wen, Phys. Rev. Lett. **96**, 110405 (2006).
[23] S. Sur and K. Yang, Phys. Rev. B **100**, 024519 (2019).
[24] T. A. Sedrakyan, V. M. Galitski, and A. Kamenev, Phys. Rev. Lett. **115**, 195301 (2015).
[25] T. A. Sedrakyan, L. I. Glazman, and A. Kamenev, Phys. Rev. B **89**, 201112(R) (2014).
[26] T. A. Sedrakyan, A. Kamenev, and L. I. Glazman, Phys. Rev. A **86**, 063639 (2012).
[27] N. Regnault and B. A. Bernevig, Phys. Rev. X **1**, 021014 (2011).
[28] E. J. Bergholtz and Z. Liu, Int. J. Mod. Phys. B **27**, 1330017 (2013).
[29] X. Wan, Z.-X. Hu, E. H. Rezayi, and K. Yang, Phys. Rev. B **77**, 165316 (2008).
[30] D. N. Sheng, Z.-C. Gu, K. Sun, and L. Sheng, Nat. Commun. **2**, 389 (2011).
[31] C. A. R. Sá de Melo, M. Randeria, and J. R. Engelbrecht, Phys. Rev. Lett. **71**, 3202 (1993).
[32] See Supplemental Material at http://link.aps.org/supplemental/10.1103/PhysRevB.109.L241113 for pertinent technical details on relevant proofs and derivations and which includes Refs. [15,24–26,38–42,46,47,50–62].
[33] K. Yang, L. K. Warman, and S. M. Girvin, Phys. Rev. Lett. **70**, 2641 (1993).
[34] O. Türker and K. Yang, Phys. Rev. B **105**, 155150 (2022).
[35] A. López, A. G. Rojo, and E. Fradkin, Phys. Rev. B **49**, 15139 (1994).
[36] J. K. Jain, Phys. Rev. B **41**, 7653 (1990).
[37] B. I. Halperin, P. A. Lee, and N. Read, Phys. Rev. B **47**, 7312 (1993).
[38] T. A. Sedrakyan, L. I. Glazman, and A. Kamenev, Phys. Rev. Lett. **114**, 037203 (2015).
[39] R. Wang, Z. Y. Xie, B. Wang, and T. Sedrakyan, Phys. Rev. B **106**, L121117 (2022).
[40] R. Wang, B. Wang, and T. A. Sedrakyan, Phys. Rev. B **105**, 054404 (2022).
[41] R. Wang, B. Wang, and T. A. Sedrakyan, Phys. Rev. B **98**, 064402 (2018).
[42] T. A. Sedrakyan, V. M. Galitski, and A. Kamenev, Phys. Rev. B **95**, 094511 (2017).
[43] The fermion density is equal to the boson density since the particle number operator remains unchanged in the transformation.
[44] P. Fulde and R. A. Ferrell, Phys. Rev. **135**, A550 (1964).
[45] A. I. Larkin and Y. N. Ovchinnikov, Sov. Phys. JETP **20**, 762 (1965).
[46] S. Gopalakrishnan, A. Lamacraft, and P. M. Goldbart, Phys. Rev. A **84**, 061604(R) (2011).
[47] C. Wei and T. A. Sedrakyan, Ann. Phys. **456**, 169354 (2023).
[48] L. Du, X. Li, W. Lou, G. Sullivan, K. Chang, J. Kono, and R.-R. Du, Nat. Commun. **8**, 1971 (2017).
[49] L. Du, I. Knez, G. Sullivan, and R.-R. Du, Phys. Rev. Lett. **114**, 096802 (2015).
[50] Z. Y. Xie, J. Chen, J. F. Yu, X. Kong, B. Normand, and T. Xiang, Phys. Rev. X **4**, 011025 (2014).
[51] G. Vidal, Phys. Rev. Lett. **98**, 070201 (2007).
[52] H. C. Jiang, Z. Y. Weng, and T. Xiang, Phys. Rev. Lett. **101**, 090603 (2008).
[53] M. Lubasch, J. I. Cirac, and M. C. Banuls, Phys. Rev. B **90**, 064425 (2014).
[54] T. Nishino and K. Okunishi, J. Phys. Soc. Jpn. **65**, 891 (1996).

[55] R. Orús and G. Vidal, Phys. Rev. B **80**, 094403 (2009).
[56] P. Corboz, T. M. Rice, and M. Troyer, Phys. Rev. Lett. **113**, 046402 (2014).
[57] J. I. Cirac, D. Poilblanc, N. Schuch, and F. Verstraete, Phys. Rev. B **83**, 245134 (2011).
[58] D. Poilblanc, N. Schuch, and I. Affleck, Phys. Rev. B **93**, 174414 (2016).
[59] S. S. Jahromi, R. Orus, M. Kargarian, and A. Langari, Phys. Rev. B **97**, 115161 (2018).
[60] G. W. Stewart, SIAM J. Matrix Anal. Appl. **23**, 601 (2002).
[61] F. Verstraete and J. I. Cirac, arXiv:cond-mat/0407066.
[62] Z. Y. Xie, H. J. Liao, R. Z. Huang, H. D. Xie, J. Chen, Z. Y. Liu, and T. Xiang, Phys. Rev. B **96**, 045128 (2017).
[63] S. Sachdev and K. Yang, Phys. Rev. B **73**, 174504 (2006).
[64] T. Devakul, V. Crépel, Y. Zhang, and L. Fu, Nat. Commun. **12**, 6730 (2021); B. R. Ortiz, S. M. L. Teicher, Y. Hu, J. L. Zuo, P. M. Sarte, E. C. Schueller, A. M. Milinda Abeykoon, M. J. Krogstad, S. Rosenkranz, R. Osborn, R. Seshadri, L. Balents, J. He, and S. D. Wilson, Phys Rev. Lett. **125**, 247002 (2020).
[65] J. Cai, E. Anderson, C. Wang, X. Zhang, X. Liu, W. Holtzmann, Y. Zhang, F. Fan, T. Taniguchi, K. Watanabe *et al.*, Nature (London) **622**, 63 (2023).
[66] H. Park, J. Cai, E. Anderson, Y. Zhang, J. Zhu, X. Liu, C. Wang, W. Holtzmann, C. Hu, Z. Liu *et al.*, Nature (London) **622**, 74 (2023).
[67] F. Xu, Z. Sun, T. Jia, C. Liu, C. Xu, C. Li, Y. Gu, K. Watanabe, T. Taniguchi, B. Tong, J. Jia, Z. Shi, S. Jiang, Y. Zhang, X. Liu, and T. Li, Phys. Rev. X **13**, 031037 (2023).
[68] Y. Xie, A. T. Pierce, J. M. Park, D. E. Parker, E. Khalaf, P. Ledwith, Y. Cao, S. H. Lee, S. Chen, P. R. Forrester *et al.*, Nature (London) **600**, 439 (2021).